

See discussions, stats, and author profiles for this publication at: <https://www.researchgate.net/publication/6953018>

# Quantum Chemical Characterization of the Structures, Thermochemical Properties, and Singlet–Triplet Splittings of Didehydroquinolinium and Didehydroisoquinolinium Ions

ARTICLE *in* THE JOURNAL OF PHYSICAL CHEMISTRY A · DECEMBER 2005

Impact Factor: 2.69 · DOI: 10.1021/jp053774g · Source: PubMed

---

CITATIONS

11

---

READS

16

3 AUTHORS, INCLUDING:



**Hilikka Kenttämää**

Purdue University

**197** PUBLICATIONS **3,077** CITATIONS

SEE PROFILE



**Christopher J Cramer**

University of Minnesota Twin Cities

**531** PUBLICATIONS **23,395** CITATIONS

SEE PROFILE

# Quantum Chemical Characterization of the Structures, Thermochemical Properties, and Singlet–Triplet Splittings of Didehydroquinolinium and Didehydroisoquinolinium Ions

John J. Nash\* and Hilkka I. Kenttämää

Department of Chemistry, Purdue University, West Lafayette, Indiana 47907

Christopher J. Cramer\*

Department of Chemistry and Supercomputing Institute, University of Minnesota, Minneapolis, Minnesota 55455

Received: July 8, 2005; In Final Form: September 7, 2005

Structural and energetic properties are predicted for the 21 didehydroquinolinium ion isomers and 21 didehydroisoquinolinium ion isomers in their lowest-energy singlet and triplet states by using density functional and multireference second-order perturbation theories. Singlet–triplet splittings and biradical stabilization energies are examined to gain insight into the degree of interaction between the biradical centers, with comparison being made to analogous didehydronaphthalenes and didehydropyridines.

## Introduction

Aromatic  $\sigma,\sigma$ -biradicals (didehydroarenes) represent a group of reaction intermediates that play an important role in the biological action of certain classes of antitumor antibiotics (e.g., enediyne). Such intermediates, produced *in vivo*, have been shown to cleave double-stranded DNA due to the ability of the biradical intermediate to abstract a hydrogen atom from each DNA strand.<sup>1</sup> Unfortunately, the extremely high reactivity of these biradicals also produces high cytotoxicity. Thus, to facilitate the development of less toxic, synthetic antitumor drugs, a better understanding of the factors that control the reactivity and selectivity of these biradical intermediates is necessary.<sup>2</sup>

The short lifetimes of such biradical intermediates in solution makes experimental studies of their chemical properties very difficult. Two of the few experimental studies in solution have shown that singlet 1,4-didehydroarenes undergo hydrogen atom abstraction reactions substantially more slowly than analogous monoradicals.<sup>3</sup> The reduced (compared to the monoradicals) reactivity of these biradicals has been proposed<sup>3a</sup> to be a result of the need for the (singlet) biradical electrons to partially uncouple in the transition state of the hydrogen atom abstraction reaction, which increases the transition state energy by an increment whose size is related to the magnitude of the singlet–triplet (S–T) splitting. For example, singlet 1,3-didehydroarenes have been suggested to be less reactive than singlet 1,4-didehydroarenes due to the larger S–T splittings for the 1,3-isomers.<sup>2a</sup> For didehydropyridine biradicals, protonation of the nitrogen atom (i.e., to generate didehydropyridinium ions) has also been proposed<sup>4</sup> to influence the S–T splittings, and consequently the reactivity, for these molecules.

Despite the interest in S–T splittings of didehydroarenes, only a few systems have been systematically examined. The S–T splittings of the three didehydrobenzenes have been predicted computationally and determined experimentally.<sup>5</sup> The compu-

tational examination of the S–T splittings of all 10 isomeric didehydronaphthalenes has provided useful insights into the spin/spin interactions in these systems.<sup>6</sup> The six isomers of the didehydropyridines have been computationally characterized,<sup>7</sup> and one isomer has been experimentally characterized by infrared spectroscopy in an argon matrix.<sup>8</sup> However, systematic studies on the S–T splittings of charged didehydroarenes are currently limited to the six protonated didehydropyridines.<sup>7c,9</sup> This lack of knowledge is puzzling, considering the fact that protonation (i.e., creation of positive charge) is one of the few factors that has been identified to influence the reactivity of biradicals. This observation is particularly intriguing since charged biradicals can be experimentally studied in the gas phase by using mass spectrometry.<sup>10</sup> Thus, to better understand the effects of charge and the presence (or absence) of heteroatoms on the structures and energetics of biradicals, we report here a systematic computational characterization of all 42 isomers of protonated didehydroquinolines and protonated didehydroisoquinolines.<sup>11,12</sup>

## Computational Methods

Molecular geometries for all species were optimized at the multiconfigurational self-consistent field (MCSCF) and density functional theory (DFT) levels of theory using the correlation-consistent polarized valence-double- $\zeta$  (cc-pVDZ<sup>13</sup>) basis set.<sup>14</sup> The MCSCF calculations were of the complete active space (CASSCF) variety<sup>15</sup> and included (in the active space) the full  $\pi$  space for each molecule and, for each of the monoradicals and biradicals, the nonbonding  $\sigma$  orbital(s). The DFT calculations were of two types. Both used the gradient-corrected exchange functional of Becke,<sup>16</sup> which was combined either with the gradient-corrected correlation functional of Lee, Yang, and Parr<sup>17</sup> (BLYP) or that of Perdew et al.<sup>18</sup> (BPW91). All DFT geometries were verified to be local minima by computation of analytic vibrational frequencies, and these (unscaled) frequencies were used to compute zero-point vibrational energies (ZPVE) and 298-K thermal contributions ( $H_{298} - E_0$ ) for all species.<sup>19</sup> DFT calculations for doublet states of monoradicals, and triplet states of biradicals, employed an unrestricted formalism. Total

\* To whom correspondence should be addressed. E-mail: jnash@purdue.edu (J.J.N.); cramer@chem.umn.edu (C.J.C.).

spin expectation values for Slater determinants formed from the optimized Kohn–Sham orbitals did not exceed 0.76 and 2.03 for doublet and triplet states, respectively. For singlet biradicals, the DFT “wave function” was allowed to break spin symmetry by using an unrestricted formalism.<sup>20</sup> Total spin expectation values for Slater determinants formed from the optimized Kohn–Sham orbitals in these cases ranged widely between 0.0 and 1.0. Geometry optimization using the unrestricted formalism has been shown to give more accurate geometries for a number of relevant aromatic biradicals.<sup>5,7b,20,21</sup>

To improve the molecular orbital calculations, dynamic electron correlation was also accounted for by using multireference second-order perturbation theory (CASPT2)<sup>22,23</sup> for the MCSCF reference wave functions; these calculations were carried out for both the DFT- and MCSCF-optimized geometries. Some caution must be applied in interpreting the CASPT2 results since this level of theory is known to suffer from a systematic error proportional to the number of unpaired electrons.<sup>24</sup> In general, then, the electronic energies are of either the CASPT2/cc-pVDZ/UBPW91/cc-pVDZ, CASPT2/cc-pVDZ//UBLYP/cc-pVDZ, or CASPT2/cc-pVDZ/MCSCF/cc-pVDZ variety, and estimates of the thermodynamic quantities,  $E_0$  and  $H_{298}$ , are derived by adding to these electronic energies ZPVE and the sum of ZPVE and  $(H_{298} - E_0)$ , respectively, where the latter are derived from the DFT calculations.

Calculations were carried out for quinolinium ion, isoquinolinium ion, the 14 isomeric dehydro(iso)quinolinium ions (D(I)Qs), and the 42 isomeric didehydro(iso)quinolinium ions (DD(I)Qs). For the DD(I)Qs, separate calculations were performed for both the lowest energy singlet and triplet states. For all molecules, calculations were carried out using  $C_s$  point group symmetry.

Isotropic  $^1\text{H}$  hyperfine coupling constants in the D(I)Qs were calculated<sup>25</sup> as

$$a_{\text{H}} = (8\pi/3)g g_{\text{H}} \beta_{\text{H}} \rho(\text{H}) \quad (1)$$

where  $g$  is the electronic  $g$  factor,  $\beta$  is the Bohr magneton,  $g_{\text{H}}$  and  $\beta_{\text{H}}$  are the corresponding values for  $^1\text{H}$ , and  $\rho(\text{H})$  is the Fermi contact integral which measures the unpaired spin density at the hydrogen nucleus. The Fermi contact integral is evaluated from

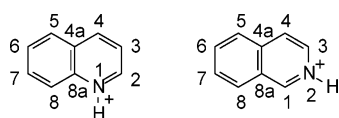
$$\rho(\text{H}) = \sum_w \mathbf{P}_{uv}^{\alpha-\beta} \phi_u(\mathbf{R}_{\text{H}}) \phi_v(\mathbf{R}_{\text{H}}) \quad (2)$$

where  $\mathbf{P}^{\alpha-\beta}$  is the UBWP91/cc-pVDZ one-electron spin density matrix, the summation runs over atomic-orbital basis functions  $\phi$ , and evaluation of the overlap between basis functions  $\phi_u$  and  $\phi_v$  is only at the hydrogen nuclear position,  $\mathbf{R}_{\text{H}}$ .

All MCSCF and DFT calculations were carried out with the MOLCAS<sup>26</sup> and Gaussian 98<sup>27</sup> electronic structure program suites, respectively.

## Results

**Geometries.** Geometric information for the biradicals, monoradicals, and related molecules, obtained using the UBWP91, UBLYP, and MCSCF methods, is provided in the Supporting Information. For the quinolinium and isoquinolinium ions, the atom numbering scheme is indicated as follows.



In general, the UBLYP geometries for quinolinium ion, isoquinolinium ion, and the singlet and triplet states of the DDQs and DDIQs are characterized by slightly longer bond lengths than the UBWP91 geometries (with the exception of meta isomers),<sup>28</sup> although the bond angles obtained using the two methods are about the same. The MCSCF geometries show shorter C–H bond lengths and slightly smaller bond angles about dehydrocarbon atoms than either of the DFT methods, but all other bond angles are about the same as those obtained using either DFT method. The MCSCF geometries also show greater localization of the aromatic  $\pi$  bonds.

For the triplet states of all 42 isomeric biradicals, the UBWP91 geometries give the lowest energies at the CASPT2 level. The calculated CASPT2 energies using either the UBLYP or the MCSCF geometries are all higher by 0.25–0.33 and 0.88–1.11 kcal/mol, respectively. This is also the case for the 14 monoradicals, quinolinium ion, and isoquinolinium ion. For these molecules, the calculated CASPT2 energies using the UBLYP and MCSCF geometries are all 0.28–0.33 and 0.96–1.10 kcal/mol, respectively, higher in energy than the energies obtained using the UBWP91 geometries. Thus, at the CASPT2 level, the UBWP91 geometries are to be preferred for the triplet states of the biradicals, as well as the doublet states of the monoradicals and the singlet states of the parent ions.

With the exception of three of the biradicals (2,4-DDQ, 6,8-DDQ, and 5,7-DDIQ) where the MCSCF geometry yields the lowest energy at the CASPT2 level, similar trends are observed for the singlet states of these molecules. For example, the CASPT2 energies using the UBLYP and MCSCF geometries all lie 0.13–0.55 and 0.15–1.75 kcal/mol, respectively, higher in energy than the CASPT2 energies obtained using the UBWP91 geometries.

The high quality of UBWP91/cc-pVDZ geometries, in general, has been noted before.<sup>7b,9,20c,21a,29</sup> It derives in part from canceling errors associated with the approximate functional and the relatively modest basis set size.<sup>30</sup> This favorable cancellation of errors makes UBWP91/cc-pVDZ a very economical choice for computing aromatic biradical structures. In any case, on the basis of these observations, we will focus any discussion of geometrical data primarily on results obtained at the UBWP91 level, unless consideration of other geometries provides additional useful information.

**Thermochemical Data.** Electronic energies and selected thermochemical quantities were computed for the 21 isomeric DDQs, the 21 isomeric DDIQs, the 7 isomeric DQs, the 7 isomeric DIQs, quinolinium ion, and isoquinolinium ion using the UBLYP and UBWP91 density functional models, as well as the CASPT2 method, in conjunction with the cc-pVDZ basis set.

ZPVEs and 298-K thermal contributions to the enthalpy were computed for each molecule from the unscaled vibrational frequencies determined at either the UBWP91 or the UBLYP level. ZPVEs and 298-K thermal contributions are provided as Supporting Information. Results from the UBLYP calculations were combined with the CASPT2/cc-pVDZ/MCSCF/cc-pVDZ total energies to derive 0-K energies,  $E_0$ , for that level for each DD(I)Q singlet and triplet state. For the DDQs, all energies are listed in Table 1 relative to the singlet state of the 7,8-isomer, and for the DDIQs, all energies are listed in Table 2 relative to the singlet state of the 5,6-isomer (each case being the respective global minimum relative to all other didehydroisomers and states).

Tables 3 and 4 list the singlet–triplet splittings,  $\Delta E_{\text{S-T}}$ , given by  $[E_0(\text{singlet}) + (H_{298} - E_0)] - [E_0(\text{triplet}) + (H_{298} - E_0)]$ ,

**TABLE 1: Relative State Energies (kcal/mol) for *m,n*-Didehydroquinolinium Ions**

	2,3	2,4	2,5	2,6	2,7	2,8	3,4	3,5	3,6	3,7	3,8	4,5	4,6	4,7	4,8	5,6	5,7	5,8	6,7	6,8	7,8
Relative $E_0$ (UBPW91/UBPW91) <sup>a</sup>																					
singlet	14.7	5.8	30.0	29.7	27.7	29.7	5.3	30.3	28.7	29.8	30.3	27.5	26.8	26.9	22.8	2.8	4.5	25.7	3.6	9.4	0.0 <sup>b</sup>
triplet	38.2	32.8	29.9	30.0	29.9	30.2	38.0	30.6	30.6	30.0	30.1	28.5	27.5	26.8	28.9	35.5	30.1	28.9	33.8	29.8	35.4
Relative $E_0$ (UBLYP/UBLYP) <sup>c</sup>																					
singlet	14.2	11.1	31.9	31.5	29.2	31.4	5.0	32.2	30.3	31.7	32.1	29.2	28.8	29.0	24.2	2.5	9.8	26.9	3.5	13.3	0.0 <sup>d</sup>
triplet	39.7	34.7	31.8	31.8	31.9	32.0	39.7	32.4	32.6	32.0	31.9	30.6	29.5	28.8	30.8	37.3	32.2	30.9	35.6	31.8	37.2
Relative $E_0$ (CASPT2/MCSCF(12,12)) <sup>e</sup>																					
singlet	13.9	13.4	30.0	29.1	27.4	29.7	5.0	30.2	28.4	29.4	30.7	27.9	26.6	27.0	21.7	1.8	12.0	24.8	2.7	13.0	0.0 <sup>f</sup>
triplet	36.9	32.2	29.7	29.6	29.5	30.2	36.9	30.6	30.4	29.9	30.3	28.3	27.4	26.7	28.9	34.1	29.4	28.7	32.3	29.4	34.2

<sup>a</sup> UBPW91/cc-pVDZ/UBPW91/cc-pVDZ + UBPW91/cc-pVDZ ZPVE. <sup>b</sup> Absolute energy (including ZPVE),  $-400.836917 E_h$ . <sup>c</sup> UBLYP/cc-pVDZ/UBLYP/cc-pVDZ + UBLYP/cc-pVDZ ZPVE. <sup>d</sup> Absolute energy (including ZPVE),  $-400.725307 E_h$ . <sup>e</sup> CASPT2/cc-pVDZ/MCSCF(12,12)/cc-pVDZ + UBLYP/cc-pVDZ ZPVE. <sup>f</sup> Absolute energy (including ZPVE),  $-399.694133 E_h$ .

**TABLE 2: Relative State Energies (kcal/mol) for *m,n*-Didehydroisoquinolinium Ions**

	1,3	1,4	1,5	1,6	1,7	1,8	3,4 <sup>a</sup>	3,5	3,6	3,7	3,8	4,5	4,6	4,7	4,8	5,6	5,7	5,8	6,7	6,8	7,8
Relative $E_0$ (UBPW91/UBPW91) <sup>b</sup>																					
singlet	25.9	26.4	21.2	27.5	27.6	26.9	12.0	29.8	27.3	29.7	29.9	27.8	26.9	27.9	23.1	0.0 <sup>c</sup>	7.8	23.3	1.5	2.7	0.4
triplet	34.7	31.9	30.0	27.5	28.3	29.3	38.3	30.3	29.8	30.0	29.8	29.1	27.6	27.8	29.4	33.4	28.5	27.4	31.9	27.8	33.7
Relative $E_0$ (UBLYP/UBLYP) <sup>d</sup>																					
singlet	26.8	26.8	21.9	29.6	29.4	28.1	11.7	31.7	28.9	31.7	31.9	29.5	29.0	30.0	24.4	0.0 <sup>e</sup>	13.1	24.4	1.6	8.1	0.3
triplet	36.7	33.9	32.0	29.6	30.4	31.3	40.3	32.4	32.0	32.2	31.9	31.2	29.7	29.9	31.4	35.5	30.8	29.6	34.0	30.2	35.9
Relative $E_0$ (CASPT2/MCSCF(12,12)) <sup>f</sup>																					
singlet	23.5	26.0	21.9	28.1	28.3	28.3	12.5	30.3	27.7	29.8	30.5	29.3	27.7	29.0	22.9	0.0 <sup>g</sup>	13.0	22.8	1.5	10.6	0.4
triplet	34.6	32.4	30.3	28.1	28.9	29.5	38.0	30.9	29.9	30.4	30.3	29.9	28.5	28.7	30.2	32.9	28.8	27.8	31.3	28.0	33.2

<sup>a</sup> At the UBLYP/cc-pVDZ level (only), the planar structure ( $C_s$ ) for the triplet state of this isomer was found to lie 0.046 kcal/mol higher in energy than a nonplanar ( $C_1$ ) structure. In this case, the ZPVE and thermal contribution were calculated using the nonplanar structure, but the CASPT2 calculations used the planar structure. <sup>b</sup> UBPW91/cc-pVDZ/UBPW91/cc-pVDZ + UBPW91/cc-pVDZ ZPVE. <sup>c</sup> Absolute energy (including ZPVE),  $-400.834065 E_h$ . <sup>d</sup> UBLYP/cc-pVDZ/UBLYP/cc-pVDZ + UBLYP/cc-pVDZ ZPVE. <sup>e</sup> Absolute energy (including ZPVE),  $-400.722789 E_h$ . <sup>f</sup> CASPT2/cc-pVDZ/MCSCF(12,12)/cc-pVDZ + UBLYP/cc-pVDZ ZPVE. <sup>g</sup> Absolute energy (including ZPVE),  $-399.692695 E_h$ .

**TABLE 3: Calculated S–T Splittings (kcal/mol) and Corresponding Doublet hfs Values (G) for *m,n*-Didehydroquinolinium Ions<sup>a</sup>**

geometry	2,3	2,4	2,5	2,6	2,7	2,8	3,4	3,5	3,6	3,7	3,8	4,5	4,6	4,7	4,8	5,6	5,7	5,8	6,7	6,8	7,8
UBPW91 <sup>b</sup>	−23.5	−27.1	0.1	−0.3	−2.2	−0.5	−32.7	−0.3	−1.9	−0.2	0.2	−1.0	−0.7	0.1	−6.0	−32.7	−25.6	−3.2	−30.2	−20.4	−35.4
UBLYP <sup>c</sup>	−25.6	−23.7	0.1	−0.4	−2.7	−0.6	−34.8	−0.3	−2.3	−0.2	0.2	−1.3	−0.7	0.2	−6.6	−34.8	−22.4	−3.9	−32.1	−18.5	−37.2
MCSCF(12, 12) <sup>c</sup>	−22.3	−18.9	0.3	−0.5	−2.1	−0.4	−32.0	−0.4	−2.0	−0.5	0.4	−0.4	−0.8	0.3	−7.2	−32.3	−17.5	−3.9	−29.6	−16.2	−34.8
<sup>1</sup> H hfs <sup>d</sup>																					
	11.2	6.2	−0.2	0.4	0.9	0.2	17.3	0.3	0.8	0.3	−0.2	−0.1	0.5	−0.1	3.3	17.2	5.7	1.8	14.8	4.7	18.2
$\Delta E_{S-T}$ ( <i>m,n</i> -Didehydronaphthalene) <sup>c,e</sup>																					
	−28.7	−17.4	0.4	−0.7	−1.9	−0.7	−32.5	−0.7	−1.9	−0.7	0.4	0.0	−0.7	0.4	−7.5	−32.5	−17.4	−5.0	−28.7	−17.4	−32.5

<sup>a</sup> Geometries optimized using the cc-pVDZ basis set. <sup>b</sup> Corrected for ZPVE differences at 298 K using the UBPW91 frequencies. <sup>c</sup> Corrected for ZPVE differences at 298 K using the UBLYP frequencies. <sup>d</sup> Isotropic hfs calculated at the UBPW91/cc-pVDZ level of theory. <sup>e</sup> Calculated at the CASPT2/cc-pVDZ/MCSCF(12,12)/cc-pVDZ level of theory.

**TABLE 4: Calculated S–T Splittings (kcal/mol) and Corresponding hfs Values (G) for *m,n*-Didehydroisoquinolinium Ions<sup>a</sup>**

geometry	1,3	1,4	1,5	1,6	1,7	1,8	3,4	3,5	3,6	3,7	3,8	4,5	4,6	4,7	4,8	5,6	5,7	5,8	6,7	6,8	7,8
UBPW91 <sup>b</sup>	−8.8	−5.4	−8.8	0.0	−0.7	−2.4	−26.3	−0.6	−2.5	−0.4	0.1	−1.3	−0.7	0.1	−6.3	−33.4	−20.6	−4.2	−30.4	−25.1	−33.3
UBLYP <sup>c</sup>	−10.1	−7.0	−10.1	0.0	−1.0	−3.2	−28.6	−0.7	−3.1	−0.5	0.1	−1.7	−0.8	0.1	−7.1	−35.5	−17.6	−5.1	−32.4	−22.0	−35.5
MCSCF(12, 12) <sup>c</sup>	−11.3	−6.3	−8.5	0.1	−0.6	−1.2	−25.6	−0.6	−2.3	−0.6	0.2	−0.5	−0.8	0.3	−7.3	−32.9	−15.7	−5.0	−29.9	−17.4	−32.7
<sup>1</sup> H hfs <sup>d</sup>																					
	4.2	2.5	3.6	−0.1	0.4	0.1	13.5	0.4	0.9	0.4	−0.1	−0.1	0.5	−0.2	3.2	17.4	4.9	2.3	14.8	5.3	17.5
$\Delta E_{S-T}$ ( <i>m,n</i> -Didehydronaphthalene) <sup>c,e</sup>																					
	−17.4	−5.0	−7.5	0.4	−0.7	0.0	−32.5	−0.7	−1.9	−0.7	0.4	0.0	−0.7	0.4	−7.5	−32.5	−17.4	−5.0	−28.7	−17.4	−32.5

<sup>a</sup> Geometries optimized using the cc-pVDZ basis set. <sup>b</sup> Corrected for ZPVE differences at 298 K using the UBPW91 frequencies. <sup>c</sup> Corrected for ZPVE differences at 298 K using the UBLYP frequencies. <sup>d</sup> Isotropic hfs calculated at the UBPW91/cc-pVDZ level of theory. <sup>e</sup> Calculated at the CASPT2/cc-pVDZ/MCSCF(12,12)/cc-pVDZ level of theory.

obtained with the three different levels of theory for the DD-(I)Qs. The CASPT2/cc-pVDZ/MCSCF/cc-pVDZ values of  $\Delta E_{S-T}$  for the corresponding didehydronaphthalenes are provided for comparison—the didehydronaphthalenes are isoelectronic with the DDQs and DDIQs but do not incorporate a protonated nitrogen atom in the aromatic system. Also included in Tables 3 and 4 are UBPW91-computed <sup>1</sup>H hyperfine coupling

constants for the corresponding monoradicals, where the given coupling is for the hydrogen atom that would need to be removed in order to generate the particular didehydro(iso)-quinolinium ion listed. In all cases, the number is the average of the two possibilities, e.g., for 2,3-DDQ, it is the average of the hyperfine splitting (hfs) for proton 2 of the 3-DQ and proton 3 of the 2-DQ. Plots of the CASPT2/cc-pVDZ/MCSCF(12,-



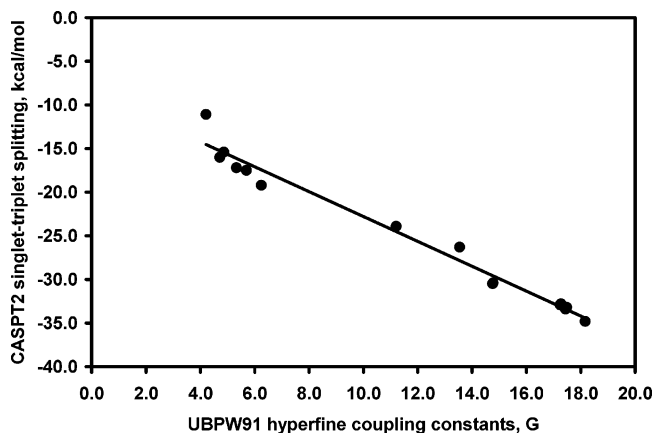


**Figure 1.** CASPT2/cc-pVDZ/MCSCF(12,12)/cc-pVDZ singlet–triplet splittings (kcal/mol) vs UBWP91-computed  $^1\text{H}$  hyperfine coupling constants (G) for *ortho*- and *meta*-DD(I)Qs.

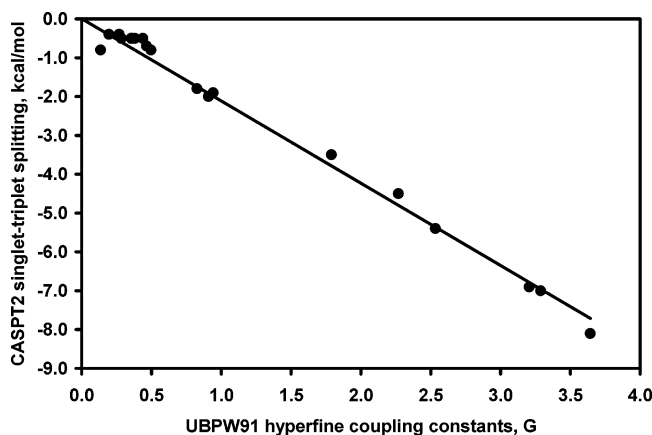
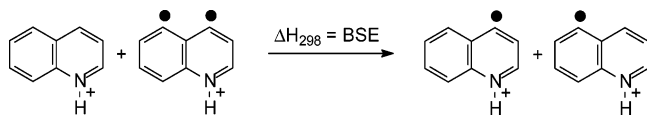


**Figure 2.** CASPT2/cc-pVDZ/MCSCF(12,12)/cc-pVDZ singlet–triplet splittings (kcal/mol) vs UBWP91-computed  $^1\text{H}$  hyperfine coupling constants (G) for DD(I)Qs (excluding *ortho*- and *meta*-DD(I)Qs).

12)/cc-pVDZ S–T splittings vs the UBWP91-computed  $^1\text{H}$  hyperfine coupling constants for the corresponding monoradicals for *ortho*- and *meta*-DD(I)Qs are shown in Figure 1, whereas all other DD(I)Qs are shown in Figure 2.

Finally, a useful perspective on the relative thermodynamic stabilities of the DD(I)Qs derives from consideration of the enthalpy changes for the isodesmic hydrogen-transfer reactions from (iso)quinolinium ion to a (iso)quinolinium ion biradical to give the two corresponding monoradical ions.



The enthalpy changes associated with these isodesmic reactions are termed the biradical stabilization energies (BSEs), as they provide a direct indication of the stabilization ( $\text{BSE} > 0$ ) or destabilization ( $\text{BSE} < 0$ ) involved when both radical sites are present in the same molecule. BSE values were computed at the three different levels of theory for the singlet and triplet states of each DD(I)Q from the 298 K enthalpies in Tables 1–2 and are listed in Tables 5 and 6 along with the corresponding CASPT2 values for the didehydronaphthalenes, for comparison.

## Discussion

Tables 1–6, with few exceptions, show near quantitative agreement between the two DFT levels and the CASPT2 level

for the relative energies and S–T splittings of all isomers. Our focus here is not to dissect the performance of the various theoretical levels but rather to assess qualitative differences (if any) between the DD(I)Qs and the isoelectronic didehydronaphthalenes (DDNs). Comparison to the didehydropyridinium ions (DDPs) is also interesting insofar as these two groups of molecules differ by benzannulation. We address these chemical issues next and defer any discussion of theoretical issues to the end of this article. Given the relative similarities among the different levels of theory, we have chosen to simplify our discussion by restricting ourselves in general to making comparisons of thermochemical properties between molecules at a single level of theory, namely, the CASPT2/cc-pVDZ//MCSCF/cc-pVDZ level (the CASPT2 energies are not very sensitive to the geometry chosen, i.e., MCSCF or DFT; the quantitative details may be found in the Supporting Information). Finally, we note that it is not possible to calculate heats of formation for the DD(I)Qs due to the lack of appropriate experimental reference data for the monoradicals found in the BSE isodesmic equations.

**Comparison to Didehydronaphthalenes.**<sup>6</sup> The quinolinium ion and isoquinolinium ion feature bond alternation similar to that observed for naphthalene. Not surprisingly, the greatest structural differences between naphthalene and either quinolinium ion or isoquinolinium ion occur around the protonated nitrogen atom. For example, the C–N bonds for quinolinium ion and isoquinolinium ion are 0.04–0.06 Å shorter than the corresponding C–C bonds in naphthalene. The C–C bonds adjacent to the C–N bonds are also shortened, but only by about 0.01–0.02 Å, and there is little to no difference in bond lengths for all of the other C–C bonds (compared to naphthalene). For quinolinium ion and isoquinolinium ion, the C–N–C bond angle is about 3.1–3.4° larger than the corresponding C–C–C bond angle in naphthalene, but all other bond angles are within about 1.5° of those in naphthalene. Thus, the influence of the protonated nitrogen atom on the structures of these molecules appears to be quite localized.

To compare the computed thermochemical properties of the DD(I)Qs with the DDNs, it was necessary to repeat the calculations for the DDNs originally reported by Cramer and Squires.<sup>6</sup> This was essential for three reasons. First, the CASPT2 calculations performed by these authors included a frozen-core approximation (which was not used for the DD(I)Q calculations). Second, these authors did not employ broken-spin-symmetry DFT calculations for the singlet states of the DDNs (which were used for the DD(I)Qs); the use of broken-spin-symmetry wave functions leads to significantly larger (i.e., more positive) ZPVEs for the singlet states of these molecules. Finally, the ZPVEs and 298-K thermal contributions to the enthalpy computed by Cramer and Squires were derived from vibrational frequencies determined at the UBWP91/cc-pVDZ level of theory; for the DD(I)Qs, these quantities were calculated at the UBLYP/cc-pVDZ level of theory.

With the exception of 3,4-DDIQ, the computed BSEs for the triplet states of the DD(I)Qs (Tables 5 and 6) all lie within 0.0–0.8 kcal/mol of those for the corresponding DDNs (the BSE for 3,4-DDIQ differs by 1.4 kcal/mol from that for 1,2-DDN). Moreover, with only four exceptions (2,3-DDQ, 4,7-DDQ, 5,8-DDQ, and 6,8-DDQ) from the 21 DDQs and three exceptions (1,3-DDIQ, 3,4-DDIQ, and 5,7-DDIQ) from the 21 DDIQs, the BSEs for the triplet DDNs are either equal to, or slightly more positive (i.e., the DDN is more stable), than the corresponding DD(I)Q. The largest differences in BSEs between the DD(I)Qs and DDNs occur for the *ortho* isomers. However, only for 2,3-

**TABLE 5: Biradical Stabilization Energies (kcal/mol) for *m,n*-Didehydroquinolinium Ions<sup>a</sup>**

geometry	state	2,3	2,4	2,5	2,6	2,7	2,8	3,4	3,5	3,6	3,7	3,8	4,5	4,6	4,7	4,8	5,6	5,7	5,8	6,7	6,8	7,8
UBPW91 <sup>b</sup>	T	-5.7	-3.3	0.0	-0.3	-0.6	-0.5	-8.0	-0.3	-0.6	-0.3	0.0	-1.2	-0.4	0.0	-1.8	-8.1	-3.1	-1.5	-7.0	-2.6	-8.5
UBLYP <sup>c</sup>		-5.5	-3.4	-0.1	-0.4	-0.7	-0.5	-7.9	-0.3	-0.7	-0.4	-0.1	-1.3	-0.4	-0.1	-1.8	-8.0	-3.3	-1.6	-6.8	-2.8	-8.4
MCSCF <sup>c</sup>		-4.6	-2.8	0.0	-0.3	-0.6	-0.4	-6.8	-0.3	-0.5	-0.3	0.0	-0.9	-0.4	0.0	-1.4	-6.9	-2.6	-1.0	-5.9	-2.1	-7.2
<i>m,n</i> -Didehydronaphthalene <sup>c,d</sup>																						
MCSCF	T	-5.1	-2.4	0.1	-0.3	-0.3	-0.3	-6.6	-0.3	-0.3	-0.3	0.1	-0.3	-0.3	-0.3	-1.2	-6.6	-2.4	-1.1	-5.1	-2.4	-6.6
UBPW91 <sup>b</sup>	S	17.8	23.9	-0.1	0.0	1.6	0.0	24.7	0.0	1.4	-0.1	-0.2	-0.2	0.2	-0.1	4.3	24.6	22.6	1.7	23.2	17.8	26.9
UBLYP <sup>c</sup>		20.0	20.3	-0.2	0.0	2.0	0.1	26.8	-0.1	1.6	-0.1	-0.2	0.0	0.2	-0.2	4.8	26.8	19.2	2.4	25.3	15.7	28.8
MCSCF <sup>c</sup>		18.5	16.1	-0.3	0.2	1.5	0.0	25.2	0.1	1.5	0.2	-0.3	-0.5	0.4	-0.3	5.8	25.4	14.9	2.9	23.7	14.1	27.0
<i>m,n</i> -Didehydronaphthalene <sup>c,d</sup>																						
MCSCF	S	23.6	14.9	-0.3	0.4	1.6	0.4	25.9	0.4	1.6	0.4	-0.3	-0.3	0.4	0.4	6.2	25.9	14.9	3.9	23.6	14.9	25.9

<sup>a</sup> Geometries optimized using the cc-pVDZ basis set. <sup>b</sup> Corrected for ZPVE differences at 298 K using the UBPW91 frequencies. <sup>c</sup> Corrected for ZPVE differences at 298 K using the UBLYP frequencies. <sup>d</sup> Calculated at the CASPT2/cc-pVDZ/MCSCF(12,12)/cc-pVDZ level of theory.

**TABLE 6: Biradical Stabilization Energies (kcal/mol) for *m,n*-Didehydroisoquinolinium Ions<sup>a</sup>**

geometry	state	1,3	1,4	1,5	1,6	1,7	1,8	3,4	3,5	3,6	3,7	3,8	4,5	4,6	4,7	4,8	5,6	5,7	5,8	6,7	6,8	7,8
UBPW91 <sup>b</sup>	T	-2.7	-1.8	-1.9	-0.1	-0.5	-1.4	-6.5	-0.4	-0.6	-0.3	-0.1	-1.2	-0.4	0.0	-1.7	-8.2	-2.7	-1.7	-6.9	-2.8	-8.2
UBLYP <sup>c</sup>		-2.9	-2.0	-1.9	-0.2	-0.5	-1.5	-6.4	-0.5	-0.6	-0.3	-0.1	-1.3	-0.5	-0.1	-1.8	-8.1	-2.9	-1.8	-6.8	-3.0	-8.2
MCSCF <sup>c</sup>		-2.2	-1.2	-1.4	-0.1	-0.3	-0.8	-5.2	-0.3	-0.4	-0.3	0.0	-0.7	-0.3	0.0	-1.3	-7.0	-2.2	-1.1	-5.9	-2.4	-7.0
<i>m,n</i> -Didehydronaphthalene <sup>c,d</sup>																						
MCSCF	T	-2.4	-1.1	-1.2	0.1	-0.3	-0.3	-6.6	-0.3	-0.3	-0.3	0.1	-0.3	-0.3	0.1	-1.2	-6.6	-2.4	-1.1	-5.1	-2.4	-6.6
UBPW91 <sup>b</sup>	S	6.1	3.6	6.9	-0.2	0.3	1.0	19.8	0.2	1.9	0.1	-0.2	0.1	0.3	-0.2	4.5	25.2	17.9	2.5	23.5	22.3	25.1
UBLYP <sup>c</sup>		7.2	5.0	8.1	-0.2	0.5	1.7	22.1	0.3	2.4	0.1	-0.2	0.4	0.3	-0.2	5.3	27.4	14.7	3.3	25.6	19.0	27.3
MCSCF <sup>c</sup>		9.1	5.1	7.1	-0.2	0.3	0.4	20.3	0.3	1.9	0.3	-0.2	-0.2	0.5	-0.3	6.0	25.9	13.5	3.9	24.0	15.0	25.7
<i>m,n</i> -Didehydronaphthalene <sup>c,d</sup>																						
MCSCF	S	14.9	3.9	6.2	-0.3	0.4	-0.3	25.9	0.4	1.6	0.4	-0.3	-0.3	0.4	-0.3	6.2	25.9	14.9	3.9	23.6	14.9	25.9

<sup>a</sup> Geometries optimized using the cc-pVDZ basis set. <sup>b</sup> Corrected for ZPVE differences at 298 K using the UBPW91 frequencies. <sup>c</sup> Corrected for ZPVE differences at 298 K using the UBLYP frequencies. <sup>d</sup> Calculated at the CASPT2/cc-pVDZ/MCSCF(12,12)/cc-pVDZ level of theory.

DDQ and 3,4-DDIQ, where the dehydrocarbon atoms are adjacent to the nitrogen atom, are the BSEs slightly more positive than the corresponding DDNs (by 0.5 and 1.4 kcal/mol, respectively). An analysis of the geometries for 2,3-DDQ and 3,4-DDIQ relative to the corresponding DDNs suggests no special structural factors contributing to these predicted differences in stability. Thus, the (relative) stabilization of the triplet states for 2,3-DDQ and 3,4-DDIQ probably results from delocalization of electron density from the dehydrocarbon atoms to the nitrogen atom. In general, then, even though the introduction of a protonated nitrogen atom into the naphthalene ring system tends to destabilize the biradical triplet states, and has the greatest effect on the triplet states of ortho isomers, these effects are very small.

With the exception of 2,3-DDQ, the computed BSEs for the singlet states of the DDQs (Table 5) all lie within 0.0–1.2 kcal/mol of those for the corresponding DDNs (the BSE for 2,3-DDQ differs by 5.1 kcal/mol from that for 2,3-DDN). In addition, with only 3 exceptions (2,4-DDQ, 6,7-DDQ, and 7,8-DDQ) from the 16 DDQs, the BSEs for the DDNs are either equal to, or are slightly more positive (i.e., the DDN is more stable), than the corresponding DDQ, which indicates that the biradical singlet states tend also to be slightly destabilized by the introduction of a protonated nitrogen atom into the ring system. Interestingly, the BSE for the singlet state of 2,3-DDQ is 5.1 kcal/mol *smaller* than that for 2,3-DDN (i.e., 2,3-DDQ is significantly less stable than 2,3-DDN). Cramer and Debbert have reported<sup>9</sup> a similar effect for 2,3-didehydropyridinium ion (2,3-DDP)—at the CCSD(T)/cc-pVDZ/UBPW91/cc-pVDZ level of theory, the BSE for the singlet state of 2,3-DDP was calculated to be 8.7 kcal/mol smaller than that for *o*-benzynes and 6.3 kcal/mol smaller than that for 3,4-didehydropyridinium ion (3,4-DDP). Because no special structural factors contribute to the predicted difference in stability, these authors postulated that “inductive effects in the cationic system play a role in charge

stabilization of similar magnitude to  $\pi$ -delocalization effects” and that “changing the formal hybridization at the 2-position from  $sp^2$  to the more electronegative  $sp$  destabilizes the 2,3-isomer relative to the 3,4-isomer”. An analysis of the structures for 2,3-DDQ and 2,3-DDN indicates that, like 2,3-DDP, there are no special structural factors that contribute to the computed difference in stability. This is also the case for the singlet state of 3,4-DDIQ (same relative positioning of the nitrogen atom and the dehydrocarbon atoms as 2,3-DDQ), which has a computed BSE that is 5.6 kcal/mol *smaller* than that for 1,2-DDN. Thus, it appears that charge stabilization via inductive effects is also responsible for destabilizing the singlet states of the 2,3-DDQ and 3,4-DDIQ isomers.

For the singlet states of the DDIQs, with the exception of 1,3-DDIQ and 3,4-DDIQ (vide infra), the computed BSEs (Table 6) lie within 0.0–1.4 kcal/mol of those for the corresponding DDNs. Interestingly, however, the BSEs for the DDNs are either equal to, or slightly more positive, than only about half of the corresponding DDIQs. For 1,3-DDIQ, the calculated BSE is 5.8 kcal/mol *smaller* than that for the corresponding 1,3-DDN (i.e., 1,3-DDIQ is significantly less stable than 1,3-DDN). Even though the separation between the dehydrocarbon atoms is somewhat smaller for 1,3-DDN (2.20 Å) than for 1,3-DDIQ (2.24 Å), it appears that the same charge stabilization effects described above for 2,3-DDQ and 3,4-DDIQ are also responsible for destabilizing the singlet state of this molecule.

With the exception of 2,3-DDQ, the computed S–T splittings for the DDQs (Table 3) lie within 0.0–2.3 kcal/mol of those for the corresponding DDNs; some of the S–T splittings for the DDQs are slightly larger than those for the corresponding DDNs, whereas others are slightly smaller. For 2,3-DDQ, the calculated S–T splitting is 6.4 kcal/mol *smaller* than that for 2,3-DDN. As described above, the triplet state for this molecule is slightly stabilized, and the singlet state is strongly destabilized (relative to the DDN), which results in a smaller S–T splitting.

**TABLE 7: ZPVEs and Calculated S–T Splittings (kcal/mol) for *m,n*-Didehydropyridinium Ions**

	2,3	2,4	2,5	2,6	3,4
	Zero-Point Energy <sup>a</sup>				
Singlet	46.7	45.9	45.4	45.6	47.0
Triplet	46.1	45.9	46.0	45.8	46.3
	S–T Splitting <sup>b</sup>				
	–23.8	–18.7	–5.5	–11.0	–31.4

<sup>a</sup> Calculated at the UBLYP/cc-pVDZ//UBLYP/cc-pVDZ level of theory; the magnitude of ( $H_{298} - E_0$ ) in every case is either 3.4 or 3.5 kcal/mol. <sup>b</sup> Calculated at the CASPT2/cc-pVDZ/MCSCF(8,8)/cc-pVDZ level of theory; corrected for ZPVE differences at 298 K using the UBLYP frequencies.

For the DDIQs, with the exception of 1,3-DDIQ and 3,4-DDIQ, the computed S–T splittings (Table 4) lie within 0.0–1.7 kcal/mol of those for the corresponding DDNs. Again, some of the S–T splittings are larger, and some are smaller, than those of the corresponding DDNs. The computed S–T splittings for 1,3-DDIQ and 3,4-DDIQ are 6.1 and 6.9 kcal/mol, respectively, smaller than those for the corresponding DDNs; however, in both cases, the reduced S–T splitting is a result of (primarily) the strong destabilization of the singlet state due to the proximity of the dehydrocarbon atoms and the protonated nitrogen atom (vide supra).

In summary, then, the introduction of a protonated nitrogen atom into the naphthalene ring system tends to destabilize both the biradical triplet and singlet states of the DD(I)Qs. While the stabilities of the triplet and singlet states, as well as the S–T splittings, are generally only affected slightly, the protonated nitrogen atom does have a quite large destabilizing influence on the singlet state for those isomers where *both* dehydrocarbon atoms are adjacent to the nitrogen atom; in these cases, the S–T splittings are significantly smaller than those for the corresponding DDNs.

**Comparison to Didehydropyridinium Ions.** All of the isomers of didehydropyridinium ion (DDP) have been studied computationally by Debbert and Cramer.<sup>9</sup> However, for the same reasons described above for the DDNs, it was necessary to repeat the CASPT2 calculations for the DDPs (Table 7) so that comparisons of thermochemical properties could be made between these molecules and the DD(I)Qs. While only a few comparisons between the DDPs and the DD(I)Qs are possible, such comparisons are useful to evaluate the effect(s) on the S–T splittings due to the presence of the additional, fused aromatic ring in the DD(I)Qs. For 2,4-DDQ, 3,4-DDQ, 1,3-DDIQ, 1,4-DDIQ, and 3,4-DDIQ, the S–T splittings are larger than those for the analogous DDPs (2,4-DDP, 3,4-DDP, 2,6-DDP, 2,5-DDP, and 2,3-DDP) by 0.2, 0.6, 0.3, 0.8, and 1.8 kcal/mol, respectively. The S–T splitting for 2,3-DDQ, however, is 1.5 kcal/mol smaller than for the analogous 2,3-DDP. For the three ortho isomers, 2,3-DDQ, 3,4-DDQ, and 3,4-DDIQ, a comparison of the dehydrocarbon atom separations in the singlet and triplet states with those for the analogous DDPs provides some insight for these differences. For the singlet states of 2,3-DDQ and 3,4-DDQ, the dehydrocarbon atom separations differ only slightly from those for 2,3-DDP and 3,4-DDP (ca. 0.006 Å longer and 0.009 Å shorter, respectively); however, the dehydrocarbon atom separations in the triplet states are markedly different (ca. 0.02 Å longer and 0.02 Å shorter, respectively). Lengthening of the C2–C3 bond in the triplet state of 2,3-DDQ decreases the overlap of the two nonbonding orbitals and stabilizes the triplet state (relative to the singlet state), which results in a smaller S–T splitting compared to 2,3-DDP. On the other hand, for 3,4-DDQ, shortening of the C3–C4 bond in the triplet state

leads to increased overlap between the two nonbonding orbitals and a larger S–T splitting compared to 3,4-DDP. For 3,4-DDIQ, the C3–C4 dehydrocarbon atom separations are smaller than those for 2,3-DDP for both the singlet (ca. 0.01 Å) and triplet states (ca. 0.02 Å). Thus, the greater overlap of the two nonbonding orbitals in the singlet state, and the lesser overlap in the triplet state, results in a larger S–T splitting compared to 2,3-DDP. These structural differences, and the resulting effects on the state splittings for the ortho isomers, clearly derive from the greater degree of bond alternation in the DD(I)Qs compared to the DDPs.

For the meta isomers, 2,4-DDQ and 1,3-DDIQ, the S–T splittings are only slightly larger than those for the analogous 2,4-DDP and 2,6-DDP (by 0.2 and 0.3 kcal/mol, respectively). While both 2,4-DDQ and 1,3-DDIQ do, in fact, show a greater degree of bond alternation than the analogous DDPs, this seems to have little effect on the S–T splittings for these molecules. For *m*-benzynes, coupling between the two nonbonding orbitals primarily occurs through space<sup>31</sup> (i.e., via overlap of the rear lobes of the two nonbonding orbitals). By consideration of the fact that the dehydrocarbon atom separations in both the singlet and triplet states of 2,4-DDQ and 1,3-DDIQ are nearly the same as those for the analogous DDPs, it is perhaps not surprising that there is very little difference in the S–T splittings for these molecules. For the para isomer, 1,4-DDIQ, the dehydrocarbon atom separations in the singlet and triplet states are also virtually identical to those for the analogous 2,5-DDP. However, for *p*-benzynes, the coupling between the two nonbonding orbitals primarily occurs through bond rather than through space.<sup>31</sup> For 1,4-DDIQ, the N2–C3 and C4a–C8a bonds are both about 0.03 Å longer than the C3–C4 and N1–C6 bonds in 2,5-DDP in both the singlet and triplet states.<sup>32</sup> Lengthening of these bonds in 1,4-DDIQ again results from the greater degree of bond alternation in this molecule compared to 2,5-DDP and serves not only to destabilize the N2–C3 and C4a–C8a  $\sigma$  orbitals but also to stabilize the corresponding  $\sigma^*$  orbitals. Thus, the lower energy antisymmetric combination of nonbonding orbitals, which couples with the  $\sigma^*$  orbitals of the N2–C3 and C4a–C8a bonds, is stabilized, whereas the higher energy symmetric combination, which couples with the corresponding  $\sigma$  orbitals, is destabilized. As a result, the S–T splitting for 1,4-DDIQ is slightly larger than that for 2,5-DDP.

To summarize this set of comparisons, the dominant effect arising from benzannulation of didehydropyridinium ion is the introduction of enhanced bond alternation into the bicyclic system, which affects the relative strengths of the various through-bond and through-space couplings manifested in the different biradicals having both dehydrocarbon atoms in the ring containing the protonated nitrogen atom.

**Geometries of *m*-DD(I)Qs.** We now examine a point where a more thoughtful analysis of theoretical models is required. The (singlet-state) potential energy surfaces for dehydrocarbon atom separation for *m*-benzynes are known to be quite flat and greatly depend on the level of theory used. Sander and co-workers have recently shown<sup>33</sup> that the UBLYP method, using either the cc-pVDZ or the cc-pVTZ basis set, gives a potential energy surface for dehydrocarbon atom separation for *m*-benzyne and 3,5-didehydropyridine that is in very good agreement with the more computationally demanding CCSD-(T)/cc-pVTZ method. Moreover, the UBLYP/cc-pVTZ calculated infrared spectra for these molecules are in excellent agreement with the experimentally determined spectra. To better understand the nature of these surfaces for the *m*-DD(I)Qs, calculations were carried out at the UBLYP/cc-pVDZ level of



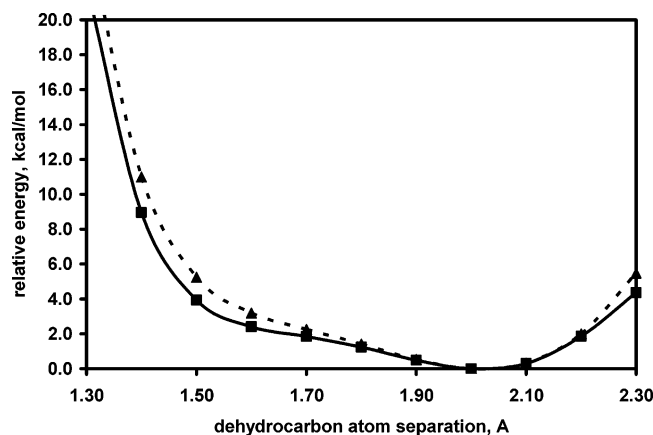


**Figure 3.** UBLYP/cc-pVDZ//UBLYP/cc-pVDZ relative energy (kcal/mol) vs dehydrocarbon atom separation (Å) for the singlet states of *m*-benzyne (▲) and 1,3-didehydronaphthalene (■).

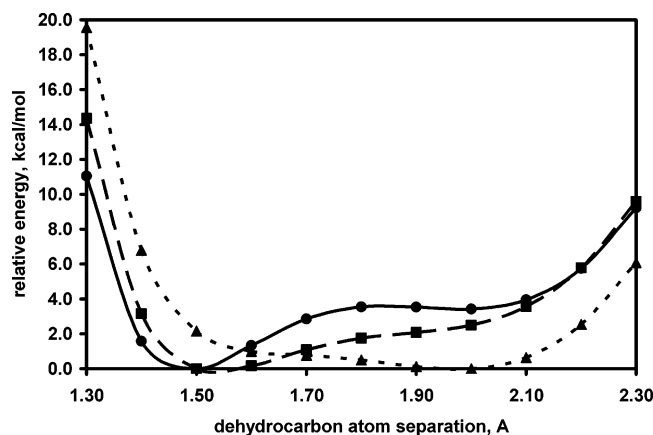


**Figure 4.** UBLYP/cc-pVDZ//UBLYP/cc-pVDZ relative energy (kcal/mol) vs dehydrocarbon atom separation (Å) for the singlet states of 2,4-DDQ (●), 5,7-DDQ (■), and 6,8-DDQ (▲).

theory, where the distance between the dehydrocarbon atoms was fixed, and all other geometric parameters were optimized.

The potential-energy surfaces for dehydrocarbon atom separation for *m*-benzyne<sup>33a</sup> and 1,3-didehydronaphthalene (Figure 3) are nearly identical at the UBLYP/cc-pVDZ level, and both show a minimum-energy structure with a dehydrocarbon atom separation of about 2.0 Å. For 2,4-DDQ and 5,7-DDQ (Figure 4), the UBLYP/cc-pVDZ calculations show an energetic preference for “closed”, tricyclic structures (over “open”, biradical structures), but the 6,8-DDQ isomer is predicted to have an open structure (although the surface is quite flat).

There is also an energetic preference for tricyclic structures for 5,7-DDIQ and 6,8-DDIQ (Figure 5), although for the 5,7-DDIQ isomer the tricyclic and open structures differ by only about 0.4 kcal/mol. The 1,3-DDIQ isomer clearly has an open structure, which is not surprising since a tricyclic structure would contain a *protonated* azirene ring with a significant amount of bond angle strain. An analysis of the geometries for 2,4-DDQ, 5,7-DDQ, and 6,8-DDQ indicates that the preference for tricyclic structures is a result of significant contributions by the resonance structures shown below. The tricyclic resonance structures permit greater charge delocalization away from the nitrogen atom into a formally aromatic cyclopropenium ion, and this delocalization is only possible for these three isomers, i.e., analogous resonance structures for 6,8-DDQ and 5,7-DDIQ do not exist. It is worth noting that these particular molecules might

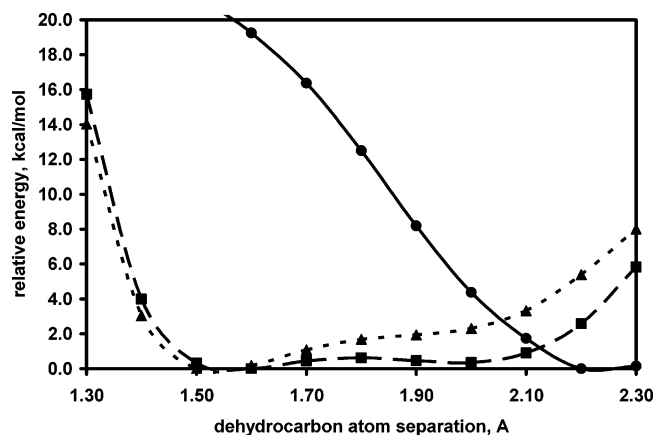
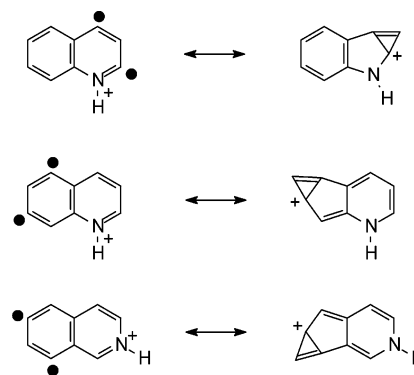


**Figure 5.** UBLYP/cc-pVDZ//UBLYP/cc-pVDZ relative energy (kcal/mol) vs dehydrocarbon atom separation (Å) for the singlet states of 1,3-DDIQ (●), 5,7-DDIQ (■), and 6,8-DDIQ (▲).

exhibit reactivity consistent with that for carbocations as opposed to more typical biradicals.



**Theoretical Disquisition.** The results presented above offer additional evidence that *unrestricted* DFT calculations provide an efficient and effective means for representing singlet aryne biradicals, even though such systems can formally have a high degree of multideterminantal character.

A separate point meriting some discussion is that a linear correlation between CASPT2/cc-pVDZ//MCSCF/cc-pVDZ S–T splittings and UBWP91/cc-pVDZ-derived proton hyperfine coupling constants has been shown to be remarkably good for a number of different types of aryne biradicals.<sup>6,7b,29,34</sup> For example, for strongly interacting *o*- and *m*-didehydroarynes (defined as having singlet ground states with S–T splittings larger in magnitude than −10 kcal/mol), the regression equation ( $R^2 = 0.997$ , 11 data points) is

$$(\text{S–T splitting, kcal/mol}) = -1.39 \times ({}^1\text{H hfs, G}) - 9.48 \quad (3)$$

whereas for less strongly interacting didehydroarynes ( $R^2 = 0.987$ , 9 data points) the correlating equation is

$$(\text{S–T splitting, kcal/mol}) = -1.99 \times ({}^1\text{H hfs, G}) - 0.30 \quad (4)$$

Note that eq 4 has a near-zero intercept, which meets with qualitative expectations that, if a proton does not “feel” any unpaired electron spin density, an electron localized in the same position would not be expected to show much preference for singlet vs triplet coupling. The reason eq 4 differs so much from eq 3 is because weakly coupled biradicals in their singlet and triplet states and the monoradicals from which they might be generated typically all have very similar geometries. Thus, unpaired spin density in the monoradical may be regarded as a



good measure of spin density from an electron at the same position in the biradical, and therefore a zero intercept for the correlating line is expected. In the strongly coupled biradicals, on the other hand, there are typically large geometry differences between the individual states of the biradicals and/or between the biradicals and the related monoradicals, which is responsible for the nonzero intercept in the correlating equation.

The correlating equations obtained for the DD(I)Qs are in very good agreement with those obtained for the other types of didehydroarynes. For the strongly interacting *o*- and *m*-DD(I)Qs, the regression equation ( $R^2 = 0.977$ , 15 data points, Figure 1) is

$$(S-T \text{ splitting, kcal/mol}) = -1.43 \times (^1\text{H hfs, G}) - 8.53 \quad (5)$$

while for the less strongly interacting DD(I)Qs ( $R^2 = 0.989$ , 27 data points, Figure 2), the correlating equation is

$$(S-T \text{ splitting, kcal/mol}) = -2.12 \times (^1\text{H hfs, G}) + 0.01 \quad (6)$$

As has been noted before, the largest errors for didehydroarynes occur either when the geometries of the singlet and triplet states are significantly different or when the (mono)radical site is adjacent to a strongly perturbing moiety such as a lone pair or a formal charge. Such effects do also manifest themselves in the DD(I)Qs. For example, the largest error (3.4 kcal/mol) is associated with 1,3-DDIQ, which has both radical sites adjacent to the formally charged nitrogen atom. Nevertheless, on the basis of eqs 5 and 6, the average error for the *o*- and *m*-DD(I)Qs is only about 0.9 kcal/mol and about 0.2 kcal/mol for all of the other DD(I)Qs. In addition, if eqs 3 and 4 are applied to the DD(I)Qs, the corresponding average errors are still quite small, 0.9 and 0.3 kcal/mol, respectively. Thus, the UBWP91/cc-pVDZ-derived proton hyperfine coupling constants continue to offer a robust and economical means with which to provide good estimates of S–T splittings in these new didehydroarynes.

## Conclusions

With few exceptions, the relative energies, S–T splittings, and biradical stabilization energies calculated at the UBLYP, UBWP91, and CASPT2 levels of theory agree quite well for the DD(I)Qs. In addition, at the CASPT2 level, the choice of geometry (i.e., UBLYP, UBWP91, or MCSCF) has little effect on the computed thermochemical properties of the DD(I)Qs, although the UBWP91 geometries consistently yield the lowest energies.

The introduction of a protonated nitrogen atom into the naphthalene ring system generally tends to destabilize both the singlet and triplet states of the DD(I)Qs, albeit only slightly. Nevertheless, for most of the DD(I)Qs, the computed thermochemical properties are remarkably similar to those for the DDNs. Only when both dehydrocarbon atoms are adjacent to the protonated nitrogen atom do the computed thermochemical properties deviate significantly from those for the DDNs. Thus, it appears that the influence exerted by the protonated nitrogen atom is quite localized.

There are also similarities between the DD(I)Qs and the DDPs (i.e., for those molecules in which both dehydrocarbon atoms reside in the ring containing the protonated nitrogen atom). Any differences between these two sets of molecules seem to be a direct result of changes in the degree of bond alternation that is introduced upon benzannulation of a DDP.

For the *m*-DD(I)Qs, ring closure to produce a tricyclic system is accentuated when such a closure permits charge transfer from the protonated nitrogen moiety to a formally aromatic cyclo-

propenium cation. In fact, certain such molecules have recently been shown<sup>35</sup> to exhibit reactivity consistent with that for carbocations as opposed to more typical biradicals.

Finally, the UBWP91/cc-pVDZ-derived proton hyperfine coupling constants continue to offer a robust and economical means with which to provide good estimates of S–T splittings in didehydroarynes.

**Acknowledgment.** We thank the National Science Foundation for financial support (CHE-0203346 and CHE-0315480).

**Supporting Information Available:** Tables of Cartesian coordinates, ZPVEs, and 298-K thermal contributions for the DD(I)Qs, D(I)Qs, quinolinium ion, and isoquinolinium ion. This material is available free of charge via the Internet at <http://pubs.acs.org>.

## References and Notes

- (1) Nicolaou, K. C.; Dai, W. M. *Angew. Chem.* **1991**, *30*, 1387.
- (2) See for example: (a) Cremer, D.; Kraka, E. *J. Am. Chem. Soc.* **2000**, *122*, 8245. (b) Chen, P. *Angew. Chem., Int. Ed. Engl.* **1996**, *33*, 1478.
- (3) (a) Schottelius, M. J.; Chen, P. *J. Am. Chem. Soc.* **1996**, *118*, 4896. (b) Roth, W. R.; Hopf, H.; Wasser, T.; Zimmerman, H.; Werner, C. *Liebigs Ann.* **1996**, 1691.
- (4) Hoffner, J.; Schottelius, M. J.; Feichtinger, D.; Chen, P. *J. Am. Chem. Soc.* **1998**, *120*, 376.
- (5) Wenthold, P. G.; Squires, R. R.; Lineberger, W. C. *J. Am. Chem. Soc.* **1998**, *120*, 5279.
- (6) Squires, R. R.; Cramer, C. J. *J. Phys. Chem. A* **1998**, *102*, 9072.
- (7) (a) Hoffner, J.; Schottelius, M. J.; Feichtinger, D.; Chen, P. *J. Am. Chem. Soc.* **1998**, *120*, 376. (b) Cramer, C. J.; Debbert, S. *Chem. Phys. Lett.* **1998**, *287*, 320. (c) Kraka, E.; Cremer, D. *J. Comput. Chem.* **2000**, *22*, 216.
- (8) Winkler, M.; Cakir, B.; Sander, W. *J. Am. Chem. Soc.* **2004**, *126*, 6135.
- (9) Debbert, S. L.; Cramer, C. J. *Int. J. Mass Spectrom.* **2000**, *201*, 1.
- (10) (a) Thoen, K. K.; Kenttämaa, H. I. *J. Am. Chem. Soc.* **1999**, *121*, 800. (b) Nelson, E. D.; Artau, A.; Price, J. M.; Tichy, S. E.; Jing, L.; Kenttämaa, H. I. *J. Phys. Chem. A* **2001**, *105*, 10155. (c) Amegayibor, S. F.; Nash, J. J.; Lee, A. S.; Thoen, J.; Petzold, C. J.; Kenttämaa, H. I. *J. Am. Chem. Soc.* **2002**, *124*, 12066.
- (11) The experimentally determined gas-phase proton affinities for quinoline and isoquinoline are 227.8 and 227.5 kcal/mol, respectively: Hunter, E. P.; Lias, S. G. *J. Phys. Chem. Ref. Data* **1998**, *27*, 413.
- (12) The conjugate bases of several of these species have also been studied computationally: Cioslowski, J.; Szarecka, A.; Moncrieff, D. *Mol. Phys.* **2003**, *101*, 1221.
- (13) Dunning, T. H. *J. Chem. Phys.* **1989**, *90*, 1007.
- (14) The choice of the cc-pVDZ basis set was made in part to facilitate comparison to prior related studies where it was demonstrated to be efficient and accurate for the prediction of thermochemical quantities such as those studied here.
- (15) Roos, B. O.; Taylor, P. R.; Siegbahn, P. E. M. *Chem. Phys.* **1980**, *48*, 157.
- (16) Becke, A. D. *Phys. Rev. A* **1988**, *38*, 3098.
- (17) Lee, C.; Yang, W.; Parr, R. G. *Phys. Rev. B* **1988**, *37*, 785.
- (18) Perdew, J. P.; Burke, K.; Wang, Y. *Phys. Rev. B* **1996**, *54*, 6533.
- (19) Several of the structures for the *m*-DD(I)Qs were found to be tricyclic using DFT methods. However, the frequencies for these molecules were still used to derive the ZPVEs and 298-K thermal contributions for the structures obtained using both DFT and MCSCF methods. There are clearly ambiguities associated with using a single level of theory to compute ZPVEs when different levels of theory provide qualitatively different structures. However, to the extent that the frequency changes that take place as a function of these different structures are expected to be associated primarily with very low frequencies (since the modes connecting the disparate structures are very soft), the energetic consequences might be expected to be small. In such an instance, using a single set of enthalpy contributions, which is functionally no different than simply comparing relative electronic energies, would appear to be reasonably well justified.
- (20) (a) Polo, V.; Kraka, E.; Cremer, D. *Theor. Chem. Acc.* **2002**, *107*, 291. (b) Gräfenstein, J.; Hjerpe, A. M.; Kraka, E.; Cremer, D. *J. Phys. Chem. A* **2000**, *104*, 1748. (c) Cramer, C. J. *J. Am. Chem. Soc.* **1998**, *120*, 6261. (d) Gräfenstein, J.; Kraka, E.; Cremer, D. *Chem. Phys. Lett.* **1998**, *288*, 593. (e) Crawford, T. D.; Kraka, E.; Stanton, J. F.; Cremer, D. *J. Chem. Phys.* **2001**, *114*, 10638.
- (21) (a) Cramer, C. J.; Nash, J. J.; Squires, R. R. *Chem. Phys. Lett.* **1997**, *277*, 311. (b) Kraka, E.; Cremer, D.; Bucher, G.; Wandel, H.; Sander,

- W. Chem. Phys. Lett.* **1997**, 268, 313. (c) Johnson, W. T. G.; Cramer, C. J. *J. Am. Chem. Soc.* **2001**, 123, 923. (d) Schreiner, P. R. *J. Am. Chem. Soc.* **1998**, 120, 4184. (e) Cramer, C. J.; Squires, R. R. *Org. Lett.* **1999**, 1, 215. (f) Sander, W.; Wandel, H.; Bucher, G.; Gräfenstein, J.; Kraka, E.; Cremer, D. *J. Am. Chem. Soc.* **1998**, 120, 8480. (g) Kraka, E.; Anglada, J.; Hjerpe, A.; Filatov, M.; Cremer, D. *Chem. Phys. Lett.* **2001**, 348, 115.
- (22) Andersson, K.; Malmqvist, P.-Å.; Roos, B. O.; Sadlej, A. J.; Wolinski, K. *J. Phys. Chem.* **1990**, 94, 5483.
- (23) Andersson, K. *Theor. Chim. Acta* **1995**, 91, 31.
- (24) Andersson, K.; Roos, B. O. *Int. J. Quantum Chem.* **1993**, 45, 591.
- (25) Lim, M. H.; Worthington, S. E.; Dulles, F. J.; Cramer, C. J. In *Density-Functional Methods in Chemistry*; Laird, B. B., Ross, R. B., Ziegler, T., Eds.; ACS Symp. Ser. No. 629; American Chemical Society: Washington, DC, 1996; p 402.
- (26) (a) Andersson, K.; Blomberg, M. R. A.; Fülischer, M. P.; Kellö, V.; Lindh, R.; Malmqvist, P.-Å.; Noga, J.; Olsen, J.; Roos, B. O.; Sadlej, A. J.; Siegbahn, P. E. M.; Urban, M.; Widmark, P.-O. *MOLCAS version 3*; University of Lund: Lund, Sweden, 1994. (b) Andersson, K.; Barysz, M.; Bernhardsson, A.; Blomberg, M. R. A.; Carissan, Y.; Cooper, D. L.; Cossi, M.; Fleig, T.; Fülischer, M. P.; Gagliardi, L.; de Graaf, C.; Hess, B. A.; Karlström, G.; Lindh, R.; Malmqvist, P.-Å.; Neogrády, P.; Olsen, J.; Roos, B. O.; Schimmelpfennig, B.; Schütz, M.; Seijo, L.; Serrano-Andrés, L.; Siegbahn, P. E. M.; Ståhring, J.; Thorsteinsson, T.; Veryazov, V.; Wierzbowska, M.; Widmark, P.-O. *MOLCAS version 5.2*; University of Lund: Lund, Sweden, 2001.
- (27) Frisch, M. J.; Trucks, G. W.; Schlegel, H. B.; Scuseria, G. E.; Robb, M. A.; Cheeseman, J. R.; Zakrzewski, V. G.; Montgomery, J. A., Jr.; Stratmann, R. E.; Burant, J. C.; Dapprich, S.; Millam, J. M.; Daniels, A. D.; Kudin, K. N.; Strain, M. C.; Farkas, O.; Tomasi, J.; Barone, V.; Cossi, M.; Cammi, R.; Mennucci, B.; Pomelli, C.; Adamo, C.; Clifford, S.; Ochterski, J.; Petersson, G. A.; Ayala, P. Y.; Cui, Q.; Morokuma, K.; Rega, N.; Salvador, P.; Dannenberg, J. J.; Malick, D. K.; Rabuck, A. D.; Raghavachari, K.; Foresman, J. B.; Cioslowski, J.; Ortiz, J. V.; Baboul, A. G.; Stefanov, B. B.; Liu, G.; Liashenko, A.; Piskorz, P.; Komaromi, I.; Gomperts, R.; Martin, R. L.; Fox, D. J.; Keith, T.; Al-Laham, M. A.; Peng, C. Y.; Nanayakkara, A.; Challacombe, M.; Gill, P. M. W.; Johnson, B.; Chen, W.; Wong, M. W.; Andres, J. L.; Gonzalez, C.; Head-Gordon, M.; Replogle, E. S.; Pople, J. A. *Gaussian 98*, rev. A.11.3; Gaussian, Inc.: Pittsburgh, PA, 2002.
- (28) We use ortho, meta, and para to refer to isomers in which the two dehydrocarbon atoms have a 1,2-, 1,3-, and 1,4-relationship, respectively, in the same ring.
- (29) Cramer, C. J.; Thompson, J. *J. Phys. Chem. A* **2001**, 105, 2091.
- (30) Gräfenstein, J.; Cremer, D. *Phys. Chem. Chem. Phys.* **2000**, 2, 2091.
- (31) Hoffmann, R.; Imamura, A.; Hehre, W. J. *J. Am. Chem. Soc.* **1968**, 90, 1499.
- (32) Elongation of the  $\sigma$  bonds would suggest a greater distance between the two dehydrocarbon atoms; however, the bond angles about the dehydrocarbon atoms also increase, which results in nearly identical dehydrocarbon atom separations in 1,4-DDIQ and 2,5-DDP.
- (33) (a) Winkler, M.; Sander, W. *J. Phys. Chem. A* **2001**, 105, 10422. (b) Winkler, M.; Cakir, B.; Sander, W. *J. Am. Chem. Soc.* **2004**, 126, 6135.
- (34) (a) Cramer, C. J.; Squires, R. R. *J. Phys. Chem. A* **1997**, 101, 9191. (b) Johnson, W. T. G.; Cramer, C. J. *J. Am. Chem. Soc.* **2001**, 123, 923. (c) Johnson, W. T. G.; Cramer, C. J. *J. Phys. Org. Chem.* **2001**, 14, 597.
- (35) Nash, J. J.; Nizzi, K. E.; Adeuya, A.; Yurkovich, M. J.; Cramer, C. J.; Kenttämaa, H. I. *J. Am. Chem. Soc.* **2005**, 127, 5760.